

Feature Alignment: Rethinking Efficient Active Learning via Proxy in the Context of Pre-trained Models

Ziting Wen¹, Oscar Pizarro^{1,2}, Stefan Williams¹

¹Australian Centre for Robotics, University of Sydney

²Department of Marine Technology, Norwegian University of Science and Technology

zwen4889@uni.sydney.edu.au, oscar.pizarro@ntnu.no, stefan.williams@sydney.edu.au

Abstract

Fine-tuning the pre-trained model with active learning holds promise for reducing annotation costs. However, this combination introduces significant computational costs, particularly with the growing scale of pre-trained models. Recent research has proposed proxy-based active learning, which pre-computes features to reduce computational costs. Yet, this approach often incurs a significant loss in active learning performance, which may even outweigh the computational cost savings. In this paper, we argue the performance drop stems not only from pre-computed features' inability to distinguish between categories of labeled samples, resulting in the selection of redundant samples but also from the tendency to compromise valuable pre-trained information when fine-tuning with samples selected through the proxy model. To address this issue, we propose a novel method called aligned selection via proxy to update pre-computed features while selecting a proper training method to inherit valuable pre-training information. Extensive experiments validate that our method significantly improves the total cost of efficient active learning while maintaining computational efficiency.

1. Introduction

Training effective deep neural networks typically requires large-scale data [11, 16, 23]. However, the high cost of acquiring data, especially annotated data, poses a significant challenge for practitioners [3, 25]. Active learning and the pretraining-finetuning paradigm are widely adopted strategies to address this challenge. Active learning reduces the demand for extensive annotation by iteratively selecting and labeling the most informative samples [28]. Additionally, the pretraining-finetuning method leverages large-scale unsupervised pre-training to create a powerful foundational model [5, 7, 14, 17], enabling exceptional performance on downstream tasks with only a limited amount of labeled

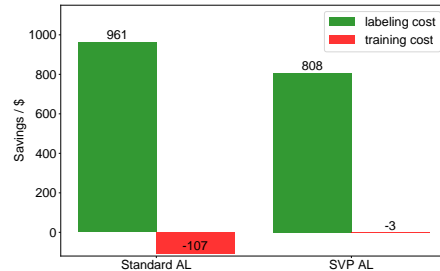


Figure 1. When achieving the accuracy equivalent to randomly selecting 100k samples through margin active learning (selecting 10k for each active learning iteration), we compared the labeling cost savings and the increased active learning training cost between standard active learning pipelines and the efficient active learning method, SVPP. We used a resnet50 model, and the training cost was priced based on AWS EC2 P3 instances (following existing paper [42]), while annotation costs were estimated using AWS Mechanical Turk¹ with triple reviews.

data. To further minimize labels' demands, researchers have naturally turned their attention to active fine-tuning, which fine-tunes the pre-training model with labeled samples selected by active learning strategies [2, 6, 37]. However, as the scale of pre-training models continues to grow [8], the training cost of active fine-tuning, which often is overlooked in traditional active learning, becomes a challenge [10].

To address this issue, recent research has introduced an efficient active learning framework known as Selection via Proxy based on pre-trained features (**SVPP**) [42]. SVPP begins by forwarding the entire dataset through a pre-trained model once, recording pre-trained features for all samples. Subsequently, in multiple iterations of active learning, a simple MLP classifier is trained using the pre-computed features for sample selection. After the sample selection, the entire model is fine-tuned once. However, we observe that, in comparison to the **standard active learning** method (fine-tuning the whole pre-trained model in each active

¹<https://aws.amazon.com/sagemaker/groundtruth/pricing/>

learning iteration), SVPP may compromise the effectiveness of active learning, resulting in additional annotation costs. As depicted in fig. 1, we noticed that while SVPP significantly reduces active learning time (training costs), its decline in active learning performance leads to a notable increase in annotation costs. Practitioners therefore have to face the hassle of weighing computational efficiency against overall cost.

In light of this challenge, in this paper, we analyze the factors contributing to the decline in active learning performance when using SVPP in sec. 4. We initially observe an intuition-aligned phenomenon: with an increase in the number of labels, fine-tuned features become more capable of distinguishing sample categories than pre-trained features. Consequently, this leads to SVPP selecting redundant samples, where redundancy refers to SVPP selecting the samples that the fine-tuned model can already predict correctly. In addition, we make an intriguing discovery: during the fine-tuning, samples selected by SVPP tend to induce more significant modifications to the pre-trained model, resulting in a decreased performance of the fine-tuned model.

Based on these insights, we propose an aligned selection via proxy strategy, **ASVP**, to enhance the performance of efficient active learning in sec. 5. First, we align the pre-computed features utilized by the proxy model with the one used in standard active learning. Specifically, we update the pre-computed features based on the fine-tuned model when the pre-trained features’ ability to distinguish sample categories significantly lags behind the fine-tuned features. In addition, we switch the training method between linear-probing then fine-tuning (LP-FT) [20] and fine-tuning (FT) to mitigate the impact of samples selected by the proxy model on the model’s performance.

Extensive experiments validate that our method notably improves the effectiveness of efficient active learning, achieving comparable or better total cost savings comparable to those of standard active learning, while still maintaining computational efficiency.

The contributions of this paper can be summarized as follows: (1) We empirically analyze the factors contributing to the performance drop when employing SVPP. The proxy model picks redundant samples where fine-tuned features outperform pre-trained ones. Also, it overlooks samples that are crucial to retain valuable pre-trained model information. (2) We propose a novel efficient active learning approach, aligned selection via proxy (ASVP), based on the above analysis. It improves the performance of efficient active learning while incurring minimal computation time. (3) We introduce a novel and practical evaluation metric for efficient active learning: the sample saving ratio. This metric directly quantifies the savings in annotation achieved by employing active learning strategies compared with the random baseline. It also facilitates the estimation of overall

savings, including savings in both computational and labeling costs, thereby assisting practitioners in making a decision on whether to use efficient active learning strategies.

2. Related Work

Active learning is a technique that minimizes the number of labels needed for model training by selectively requesting annotations for samples. Numerous active learning strategies have been proposed, primarily encompassing uncertainty sampling [13, 18, 21, 30, 36], diversity sampling (feature space coverage) [24, 31], their combinations [1, 32, 38], and some learning-based approaches [33, 34, 40]. With the advancement of large-scale unsupervised pre-training and fine-tuning, an increasing number of researchers have turned their attention to active fine-tuning, which fine-tunes the pre-trained model with samples selected by active learning strategies. Given the success of the pre-training fine-tuning mode, most works of active fine-tuning have focused on developing active learning strategies that can work with extremely limited annotations [15, 35, 39]. Furthermore, researchers have validated the performance of existing active learning methods when applied to pre-training fine-tuning mode, demonstrating that traditional margin sampling exhibits strong performance [12, 42].

Efficient active learning. Most active learning methods operate in a multi-round mode, iteratively training models and selecting samples to label. This mode entails significant training time and costs. In the context of active fine-tuning, this phenomenon becomes more pronounced, as larger models are better equipped to effectively leverage data in unsupervised pre-training [8, 26].

Increasing the active learning batch size, which refers to the number of samples selected per active learning iteration [9, 43], is one solution to enhance computational efficiency. However, it weakens the performance of active learning. Moreover, even when increasing the active learning batch size, there remains the considerable computational cost associated with training the entire network multiple times. Therefore, recent research has explored single-shot active learning based on pre-trained features [37]. However, as the number of labels increases, the effectiveness of this method gradually diminishes in comparison to other standard active learning strategies.

Another solution to boost active learning efficiency is to use less computationally intensive models or training methods as proxy tasks for sample selection, known as Selection via Proxy (SVP) [10]. Typical proxy tasks include reducing model complexity, such as using models like ResNet8 or ResNet14, early stopping, or training linear classifiers or MLPs based on pre-trained features [42]. However, these proxy tasks often have an impact on active learning performance and may result in savings in computation costs not

outweighing the increase in annotation costs. As a result, practitioners are often faced with a trade-off between computational efficiency and the overall cost.

3. Preliminary

We briefly review the Selection via Proxy framework based on pre-computed features, SVPP, as shown in fig. 2. We denote the labeled set as L , the unlabeled set as U . The pre-trained neural network backbone is defined as $f(\cdot; \theta_p) : \mathcal{X} \rightarrow \mathbb{R}^d$, where θ_p represents weights of the pre-trained model, \mathcal{X} is the data space and \mathbb{R}^d is normalized feature space. And we define the predictor as $h(\cdot; \theta_h) : \mathbb{R}^d \rightarrow \mathbb{R}^c$, where θ_h is weights of the predictor and \mathbb{R}^c is the output space. SVPP follows a three-step process. First, all samples are forward-passed through $f(\cdot; \theta_p)$, and the pre-trained features are saved. Subsequently, the proxy model is trained, and samples are selected iteratively based on the active learning strategy. In this process, the predictor $h(\cdot; \theta_h)$ serves as the proxy model, utilizing pre-computed features as its input. The final step is fine-tuning the pre-trained model $h(f(\cdot; \theta_p); \theta_h)$ based on the obtained labels.

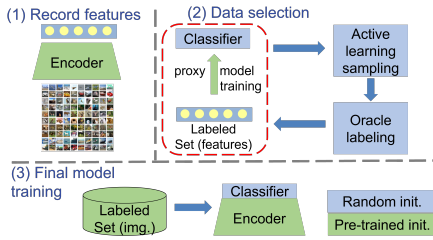


Figure 2. The Selection via Proxy based on pre-trained features (SVPP) Framework. Stage 1: pre-computing features. Stage 2: sample selection based on the proxy model (a simple classifier) with pre-computed features as input. Stage 3: Fine-tuning the pre-trained model using labeled samples.

4. Observation and Analysis

To analyze the factors contributing to the decline in SVPP active learning performance, we investigated the differences in sample selection between the fine-tuned model, $h(f(\cdot; \theta_p); \theta_h)$, and the proxy model, $h(\cdot; \theta_h)$. Our analysis is based on uncertainty sampling because uncertainty-based methods are widely employed in active learning strategies. Recent benchmarks have demonstrated uncertainty sampling as the state-of-the-art approach when fine-tuning pre-trained model [12, 42]. As illustrated in fig. 3, compared to the samples selected by the fine-tuned model, the proxy model misses samples from regions A and B while additionally selecting samples from regions C and D. Building on the rationale that adding samples already correctly predicted by the model seldom improves its performance,

whereas incorporating samples the model predicts incorrectly often leads to performance enhancements. The impact of the proxy model on active learning performance primarily stems from missing samples in region B (missing region) and selecting samples redundantly in region C (redundant region).

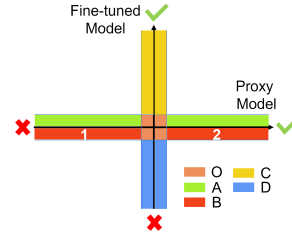


Figure 3. Sample Selection Discrepancy: Proxy vs. Fine-tuned Models. The two axes represent the confidence of predictions for the proxy model and the fine-tuned model, with the positive half-axis indicating correct predictions and the negative half-axis indicating incorrect predictions. Uncertainty-based active learning selects samples with the lowest prediction confidence, meaning the proxy model chooses samples from regions O, C, and D, while the fine-tuned model selects samples from regions O, A, and B. For convenience in further analysis, we denote the incorrect predictions made by the proxy model in region B as B1, and the correct predictions as B2. Both the proxy model and the fine-tuned model confidently predict the remaining white region, hence they do not select samples from it.

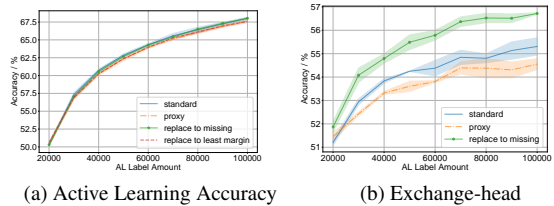


Figure 4. Comparison of exchange-head accuracy and active learning accuracy for samples selected via fine-tuned model (standard), proxy model, and replace experiment (replacing samples selected by the proxy model with those from the missing region).

Observation 1: The absence of samples from the missing region leads to a decline in the performance of the fine-tuned model. We employed one of the uncertainty-based active learning strategies, margin sampling, in three ways on the ImageNet dataset: (1) using the fine-tuned model, (2) using a proxy model, and (3) a replacement experiment where the top 20% of the samples with the largest margins in the selection of the proxy model were replaced with samples from the region B2. Additionally, considering that replacing samples with smaller margins in the fine-tuned model could potentially affect the final accuracy, we conducted another replacement experiment, replacing to least margin. In this setup, we directly replaced

the top 20% samples with the largest margins in the selection of the proxy model with samples of the smallest margin on the fine-tuned model (region A and region B). The accuracy of the fine-tuned model is illustrated in fig. 4a. Replacing samples with missing region samples shows very close active learning accuracy to that achieved based on the fine-tuned model. However, simply replacing them with samples that have the smallest margin in the fine-tuned model does not improve model accuracy.

As illustrated in fig. 3, samples in region B2 are well-distinguished in the pre-trained feature space (predicted accurately and confidently by the proxy model). However, the fine-tuned model struggles to predict these samples correctly, displaying high uncertainty in its predictions. Therefore, we speculate that replacing the samples selected by the proxy model with samples from this region improves active learning performance for the following reasons:

Potential reason: The samples selected from the missing region B2 potentially aid the fine-tuned model in retaining valuable pre-trained feature information, thereby enhancing active learning performance. We conducted exchange-head experiments to determine how much the fine-tuned model alters the feature space of the pre-trained model. Specifically, we placed the fine-tuned classifier on the pre-trained backbone to evaluate accuracy. Higher accuracy indicates less alteration of the pre-trained model by fine-tuning [29]. As shown in fig. 4b, samples chosen by the proxy model induce the most changes in the pre-trained feature space, while replacing the 20% samples selected by the proxy model with missing region samples significantly reduces alterations to the pre-trained model.

Observation 2: As the number of annotations increases, the proxy model selects more samples from redundant regions. The experiments on CIFAR-10 as shown in fig. 5a. This observation aligns with intuition: as annotations increase, the features of the fine-tuned model become more adept at distinguishing between sample categories than those of the proxy model. Consequently, there is a gradual increase in the percentage of redundant samples chosen by the proxy model in each round. This implies that, as annotations increase, the influence of sample selection from the redundant region becomes more pronounced in active learning performance.

Observation 3: The samples selected from the redundant region contribute little to improving the fine-tuned model. We conducted experiments on the CIFAR-10 dataset with margin sampling. The initial pool was set to 1000 samples, and subsequently, 1000 samples were added through (1) fine-tuning the model, (2) samples from the redundant region, and (3) random selection. The results are depicted in fig. 5b. The accuracy of adding samples from redundant regions is almost the same as that of adding samples randomly and is lower than the results obtained by se-

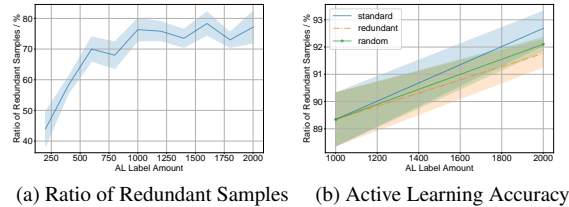


Figure 5. Observation of redundant region samples. (a) the proportion of redundant region samples among the newly added samples of each active learning round, where 10 rounds of margin sampling on CIFAR-10, selecting 200 samples per round. (b) Active learning accuracy comparison among selecting margin samples via fine-tuning, selecting samples from the redundant region, and random sample selection.

lecting samples using the fine-tuned model.

5. Method

In line with the analysis presented in sec. 4, addressing the performance drop of SVPP primarily involves focusing on the disparities between SVPP and standard active learning in redundant and missing regions. For samples in the redundant region, the fine-tuned model can predict these samples correctly with high confidence, but the proxy model struggles to differentiate them. This suggests that the features of the fine-tuned model are more suitable for distinguishing these samples. So, we suggest performing a complete model fine-tuning as the number of these samples increases, updating the pre-computed features to enhance the proxy model’s discriminative capacity for this region and, consequently, reducing the selection of redundant region samples. The data selection stage of our method is shown in fig. 6.

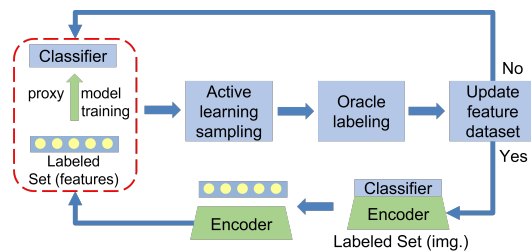


Figure 6. The Data Selection Pipeline in our approach, Aligned Selection via Proxy (ASVP). After acquiring new labels from the oracle, we assess the necessity of updating the pre-computed features. If required, the pre-trained model is fine-tuned, and the pre-computed features are subsequently updated.

For the missing region, these samples are selected to assist the fine-tuned model in preserving valuable pre-trained information as discussed in sec. 4. So, the focus should be on aiding the fine-tuned model in inheriting the ability to distinguish missing region samples from the pre-trained

model rather than selecting them. Specifically, in sec. 5.1, we describe how to determine the moment for updating pre-computed features. In sec. 5.2, we detail how to mitigate the impact of the missing samples by altering the training method of the final model.

5.1. Aligning Proxy Features

As discussed in sec. 4, with the increase in annotations, the quality of fine-tuned features improves gradually, resulting in a higher proportion of samples selected by the proxy model from the redundant region. Also, adding the samples from the redundant region rarely improves the performance of the fine-tuned model. Hence, we assess the ratio of redundant region samples by evaluating the changes in the performance of the fine-tuned model after adding more annotated samples. To assess the changes in the fine-tuned model’s performance, we employ LogME-PED [22, 41] as an indicator. LogME-PED is an evaluation metric for pre-trained models, where the LogME component estimates the pre-trained model’s capability to effectively differentiate given annotated samples, and PED, a physically inspired model, simulates feature learning dynamics through multiple iterations.

Specifically, in every active learning iteration, we first compute the PED component. If convergence is achieved within a single iteration, we infer that the fine-tuned features will maintain similarity to the pre-trained features. So, there is no need to calculate the LogME metric and update the pre-computed features. However, if the PED component converges with more than one iteration, we proceed to compute the LogME metric. When the difference between the current LogME score and that from the previous active learning iteration is below a predefined threshold, we deduce that the fixed pre-trained features pose a significant obstacle to the performance improvement of the proxy model, prompting us to fine-tune the model and update the pre-computed features.

5.2. Preserving Valuable Pre-trained Features

As speculated in sec. 4, sampling from the missing region improves model performance by reducing the alterations of the pre-trained model by fine-tuning. Based on this, we propose preserving valuable and sensitive pre-trained information by adjusting the training method of the final model, instead of trying to incorporate these samples. Specifically, after sample selection, we employ the LP-FT method [20] to train the final model. LP-FT initiates the training process by exclusively updating the linear head with frozen pre-trained weights, followed by a standard fine-tuning phase. This sequential approach is designed to minimize alterations to the pre-trained model induced by fine-tuning.

Furthermore, the missing region comprises two types of samples: those the proxy model based on pre-trained fea-

tures can correctly predict (region B2) and those it cannot (region B1). Similar to the redundant region analysis, as annotations increase, fine-tuned features outperform pre-trained ones. This leads to a gradual increase in samples from region B1 compared to region B2. In this scenario, continuing to use LP-FT may retain incorrect pre-trained information. Therefore, we also switch the model’s training method from LP-FT to FT, while updating pre-computed features.

6. Results

Our method is validated on four datasets: ImageNet-1k [11], CIFAR-10 [19], CIFAR-100 [19] and Oxford-IIIT Pet dataset [27] with four typical active learning strategies. The experiment setup is clarified in sec. 6.1. We propose the new efficient active learning evaluation metric in sec. 6.2. The results are shown in sec. 6.3 and sec. 6.4. The ablation study is shown in sec. 6.5. The detailed study of the impact of the position of updating features is shown in sec. 6.6. Additionally, given the efficiency of our framework, decreasing the amount of sample selected in each active learning iteration to alleviate the redundant problem of batch active learning strategy is feasible. The results are shown in sec. 6.7.

6.1. Experiment Setup

Active learning strategies. To evaluate the compatibility of our proposed ASVP with existing active learning strategies, four typical active learning strategies are included: (1) Margin: uncertainty-based sampling, one of the SOTA in the context of fine-tuning pre-trained models [30], (2) Confidence: uncertainty-based sampling, (3) BADGE: combination of uncertainty and diversity [1], (4) ActiveFT(al), feature space coverage with features from fine-tuned model [37].

Baseline. (1) Standard active learning: training the whole model with fine-tuning (FT) or linear-probing then fine-tuning (LP-FT) [20] in each active iteration, (2) SVPP [42]: selecting samples via MLP proxy model based on pre-trained features and training the final model with FT, (3) ActiveFT(pre) [37]: a single-shot active learning strategy that selects all sample in single iteration based on pre-trained features.

Implementations. We utilized the ResNet-50 model [16], pre-trained on ImageNet using the BYOL-eman [4] method in all our experiments. The training hyperparameters of the two model training approaches, fine-tune (FT) and LP-FT, are provided in appendix 8. For the baseline method (SVPP) and our method (ASVP), we employed 2-layer MLPs as proxy models, where its architecture is Linear + BatchNorm + ReLU + Linear. The hidden layer width matched the input feature dimensions. For the ImageNet, CIFAR-10, and Pets datasets, we

conducted 10 active learning iterations, with each iteration selecting 10,000, 200, and 200 samples, respectively. In the CIFAR-100, 15 active learning iterations were performed, with each iteration selecting 400 samples. The difference in LogME-PED scores between consecutive active learning iterations is set as 1 for the threshold of updating pre-computed features.

6.2. Metric

Efficient active learning methods often exhibit a lower accuracy compared to standard active learning approaches. Understanding the additional annotation costs needed to compensate for the accuracy gap caused by efficient active learning allows practitioners to weigh the computational cost savings against increased labeling expenses, aiding their decision to utilize these methods.

To this end, we propose a new evaluation metric: equivalent saving amount. Let N_1 represent the number of samples selected by the active learning strategy, and let A be the accuracy achieved by a model trained with these N_1 labeled samples. We utilize interpolation to estimate the number of samples, N_2 , required to achieve accuracy A for a random baseline. The number of saved samples is $N_2 - N_1$ and **sample saving ratio** is $\frac{N_2 - N_1}{N_2}$. The **overall cost** of active learning, including annotation and training costs, equals $N_1 \times P_l + C_{tr}$, where P_l denotes the unit price of annotation and C_{tr} represents the training cost of active learning. Additionally, in real-world scenarios, active learning involves multiple iterations with varying counts. We calculate the average sample saving ratio to assess the performance.

In this paper, we primarily present the average sample savings ratio, overall costs, and computational time. Additionally, detailed accuracy and the corresponding savings in sample count in each active learning iteration are provided in appendix 9.

6.3. Sample Saving Ratio and Overall Cost

The average sample savings ratios are presented in table 1, with each experimental setting repeated three times to report both the average and standard deviation. The table also illustrates the total cost required for active learning to reach the accuracy achieved by the random baseline at the last active learning iteration (i.e., the accuracy achieved when randomly selecting 100k, 2000, 6000, and 2000 samples from ImageNet, CIFAR-10, CIFAR-100, and Pets datasets, respectively). The training cost is assessed based on AWS EC2 P3 instances [42], while the annotation cost is evaluated using AWS Mechanical Turk, with three annotations per sample to ensure labeling quality. Additionally, the accuracy and corresponding saving in label counts on ImageNet with margin sampling are shown in fig. 7. The other results are shown in appendix 9.

Our method consistently outperforms the efficient active

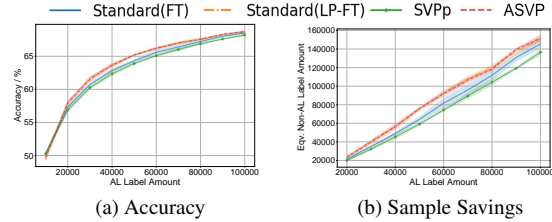


Figure 7. The accuracy and equivalent non-active learning label amounts of the standard method, SVPP and our method ASVP on the ImageNet. The equivalent non-active learning label amount refers to the number of samples selected by a random baseline to achieve the same accuracy as active learning.

learning method, SVPP, in terms of sample saving ratio and overall cost reduction. It surpasses the single-shot active learning strategy, ActiveFT(pre), when combined with most active learning strategies. In most cases, our approach offers similar or greater overall cost savings compared to standard active learning. This alleviates practitioners’ concerns about overall costs when using efficient active learning. Additionally, in standard active learning methods, the lack of a clear criterion for choosing the proper training method may lead to suboptimal results. Specifically, the standard active learning with FT outperforms the standard active learning with LP-FT on CIFAR-10 and Pets, while on ImageNet and CIFAR-100, the standard (LP-FT) method demonstrates better performance. In contrast, our approach, by switching training methods, ensures a relatively favorable performance in practical applications.

Compared to the single-shot active learning method ActiveFT(pre), our approach is compatible with various existing active learning strategies and exhibits lower dependence on the quality of pre-trained features. The reliance of ActiveFT(pre) on the quality of pre-trained features leads to suboptimal results. This is particularly evident in datasets like Pets, where the pre-trained feature quality is low.

6.4. Computational Time

We define the average model training time for both the fine-tuned model and the proxy model in each active learning iteration as $T_{tr,full}$ and $T_{tr,proxy}$, respectively. The time for processing all unlabeled samples through the whole pre-trained model and the proxy model to compute active learning metrics and select samples is denoted as $T_{f,full}$ and $T_{f,proxy}$, respectively. The time spent on forwarding all samples through the model to record features is represented by T_{pre} . The active learning iteration count is given by N_{al} . The total active learning time for standard active learning, $T_{s,full}$, is $N_{al} \times (T_{tr,full} + T_{f,full})$. The total time for SVPP, $T_{s,svpp}$, is $N_{al} \times (T_{tr,proxy} + T_{f,proxy}) + T_{pre}$. For ASVP, $T_{s,asvp}$, the total time is $N_{al} \times (T_{tr,proxy} + T_{f,proxy}) + 2 \times T_{pre} + T_{tr,full}$. When maintaining the

Selection Method	Training Method	AL Strategy	ImageNet		CIFAR-10		CIFAR-100		Pets		Cost Saving Ratio
			Avg. Sample Saving Ratio	Cost	Avg. Sample Saving Ratio	Cost	Avg. Sample Saving Ratio	Cost	Avg. Sample Saving Ratio	Cost	
Standard	FT	Random	-	3600	-	72	-	216	-	72	100%
Standard	FT	Margin	22.70±1.90	2739	42.77±1.05	44	8.86±2.25	207	31.67±2.30	48	75%
		BADGE	16.87±0.67	2962	35.95±0.78	46	8.97±2.54	212	33.01±3.17	47	77%
		Confidence	-19.82±1.05	3672	20.09±3.06	54	-5.24±3.16	226	27.24±3.28	50	88%
		ActiveFT(al)	-	-	9.32±3.43	62	3.09±0.44	379	-5.20±2.28	141	152%
Standard	LP-FT	Margin	30.97±0.51	2461	38.83±0.45	45	17.31±1.90	203	6.97±2.55	74	82%
		BADGE	24.23±1.11	2777	25.35±1.32	51	15.35±1.55	209	6.74±3.84	70	85%
		Confidence	-12.71±2.66	3636	14.69±4.65	52	4.88±4.22	229	9.58±3.41	73	95%
		ActiveFT(al)	-	-	5.38±1.81	73	8.08±0.64	478	-29.33±10.58	148	176%
Single-shot	FT	ActiveFT(pre)	-	-	-3.36±4.92	75	1.89±1.68	434	-11.92±1.26	167	170%
	LP-FT		-	-	19.58±2.21	189	10.86±1.24	410	-38.10±2.61	265	273%
SVPP	FT	Margin	16.64±2.06	2795	23.63±4.01	53	1.36±1.45	213	23.48±4.09	50	80%
		BADGE	13.01±1.36	3038	14.96±5.89	58	-2.11±0.85	376	-7.78±2.42	129	130%
		Confidence	-25.97±1.28	6756	-11.54±2.30	73	-14.43±2.49	496	2.40±7.25	67	153%
		ActiveFT(al)	-	-	-4.72±5.78	72	0.25±0.92	388	-11.63±6.85	519	333%
ASVP	FT/LP-FT	Margin	30.22±1.85	2381	35.03±1.89	49	13.31±1.86	200	21.98±0.50	49	74%
		BADGE	24.43±1.12	2727	33.67±0.84	47	8.16±1.98	208	6.10±5.59	57	79%
		Confidence	-6.37±1.23	3326	23.92±5.16	52	-0.62±1.43	362	14.81±3.17	51	100%
		ActiveFT(al)	-	-	27.45±1.42	53	11.28±2.01	217	-7.74±4.81	76	93%

Table 1. Average sample savings ratios, with each configuration repeated three times to calculate the average and standard deviation. The training method indicates how the final model is trained, and the selection method indicates the model used for sample selection. The cost refers to the total cost required for active learning to achieve the accuracy achieved by the random baseline in the last active learning iteration. The cost-saving ratio refers to the average ratio of the cost of active learning to the cost of the random baseline. The best results are shown in red and the second-best results are in blue.

same number of active learning iterations as standard active learning, the time saved by ASVP is primarily influenced by $2 \times T_{pre} + T_{tr,full}$.

	T_{pre} /hrs	$N_{al} \times T_f$ /hrs	$N_{al} \times T_{tr}$ /hrs	T_s /hrs
Standard	-	11.66	23.86	35.52
SVPP	0.92	0.07	0.11	1.10
ASVP	1.84	0.07	2.67	4.58

Table 2. Computation time comparison of various active learning sample selection methods on ImageNet using V100 GPU.

Given that the computation time of the proxy model, MLP, is significantly less than that of the fine-tuned model, ASVP also opens up the potential for increasing the number of active learning iterations. The computational times for standard active learning, SVPP, and ASVP are presented in table 2, where the running time is measured on ImageNet. Since our method achieves the same accuracy as the standard pipeline by only adopting LP-FT, the running time of ASVP is not reported based on practical running. This time is estimated based on the SVPP running time. The computational time on other datasets is shown in appendix 10.

6.5. Ablation Study

Our ablation study was conducted on CIFAR-10, CIFAR-100, and Pets and the results are presented in table 3. Additional ablation studies on other active learning strategies are provided in appendix 11. Across all three datasets, updating pre-computed features (feature alignment) consistently led to a noticeable performance boost. Meanwhile, switching training methods (training alignment) improved performance on all datasets except for the Pets dataset, suggesting that our method may not precisely determine the optimal point for switching training methods. However, considering the practical scenario where we cannot pre-determine whether using FT or LP-FT for training is better, our approach still aids in selecting a preferable training method.

6.6. Influence from Position of Updating Features

We examined the impact of the position of updating pre-computed features on CIFAR-10. The number of saved samples throughout the entire active learning iteration process is depicted in fig. 8, with the average savings ratio presented in table 4. The choice of updating pre-computed features does indeed affect the final performance of ASVP. Nevertheless, across the six different positions explored in the experiments, ASVP consistently outperforms the method relying solely on pre-training features (SVPP). Fur-

Feature alignment	Training alignment	CIFAR-10	CIFAR-100	Pets
No	No	23.63±4.01	1.36±1.45	23.48±4.09
No	Yes	24.96±2.74	7.69±1.56	18.45±3.89
Yes	No	31.42±2.65	6.98±2.03	27.01±0.51
Yes	Yes	35.03±1.89	13.31±1.86	21.98±0.50

Table 3. Ablation Study. Comparison of the average sample saving ratio of solely updating pre-computed features (training the final model using fine-tuning), solely switching training methods (using pre-trained features), and the complete ASVP approach (both updating pre-computed features and switching training methods) under different datasets with margin sampling.

thermore, our proposed method for determining the update location based on LogME-PED proves to be effective. On CIFAR-10, this method selects the update of pre-computed features at 600 labels, ranking as the second-best among the six experimental positions, as shown in table 4. The positions of updating pre-computed features estimated through LogME-PED are outlined in appendix 12.

Change at	Saving Ratio	Change at	Saving Ratio
w/o	23.63±4.01		
200	33.13±2.32	800	36.03±1.48
400	32.13±4.60	1000	32.75±1.91
600	35.03±1.89	1200	31.33±1.87

Table 4. The influence of the position of updating pre-computed feature on average sample savings ratios on CIFAR-10. The best results are shown in red and the second-best results are in blue.

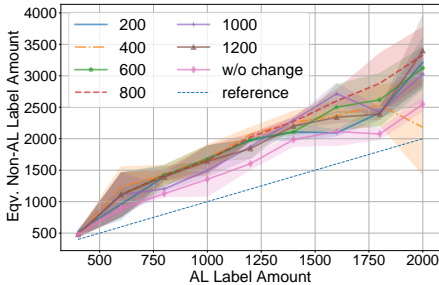


Figure 8. The impact of the position of updating pre-computed features on the savings of label amounts in CIFAR-10 across each active learning iteration. The equivalent non-active learning label amount refers to the number of samples selected by a random baseline to achieve the same accuracy as active learning

6.7. Improvement from Small Batchsize

The training costs associated with deep neural networks often lead practitioners to augment the number of samples selected per active learning iteration to ensure computational

feasibility. Unfortunately, this strategy tends to result in selecting some redundant samples. Given the efficiency of our method, we can alleviate this problem. We conducted experiments on ImageNet, randomly selecting an initial pool of 10,000 samples. Subsequently, we performed 9, 45, 180, and 900 active learning iterations using margin sampling, selecting a total of 100,000 samples. The accuracy of the final model and the total sample selection time for both FT and LP-FT training are presented in table 5. The results show a general improvement in active learning performance with an increase in the number of iterations. However, beyond 180 iterations, the performance improvement diminishes, indicating a limit to the benefits of increasing the number of active learning iterations.

Additionally, the accuracy of SVPP (final model is fine-tuned) with more active learning iterations remains lower than that of the standard active learning pipeline. However, when using LP-FT for final model training and increasing the iteration count to 45 or more, ASVP surpassed the standard active learning method in terms of accuracy.

# AL iterations	Training Method		Sampling Time / hrs
	FT	LP-FT	
9	16.64±2.06	30.22±1.85	1.1
45	17.66±1.37	31.20±0.40	1.5
180	19.43±0.86	32.00±0.46	3.7
900	18.21±0.67	31.64±0.24	15.8

Table 5. The influence of the number of active learning iterations on average sample savings ratios and sampling time on ImageNet.

7. Conclusion

Active learning on pre-trained models shows label efficiency but demands significant computational time, whereas current efficient active learning methods tend to compromise a notable fraction of active learning performance, resulting in increased overall costs. To address this challenge, this paper attributes the reduced performance of SVPP to (1) the absence of samples necessary for preserving valuable pre-trained information and (2) an increased selection of redundant samples due to fine-tuned features becoming better than pre-trained features as the annotation increases. Building upon this analysis, we propose ASVP, a two-fold alignment approach to improve the effectiveness of the efficient active learning method with similar or marginally increased computational time. Additionally, we introduce the sample savings ratio as a metric to assess the effectiveness of efficient active learning, providing a straightforward measure for labeling cost savings. Experiments show that our proposed ASVP saves similar or greater total costs in most cases, while still maintaining computational efficiency.

References

- [1] Jordan T. Ash, Chicheng Zhang, Akshay Krishnamurthy, John Langford, and Alekh Agarwal. Deep batch active learning by diverse, uncertain gradient lower bounds. In *International Conference on Learning Representations*, 2020. [2](#), [5](#)
- [2] Javad Zolfaghari Bengar, Joost van de Weijer, Bartłomiej Twardowski, and Bogdan Raducanu. Reducing label effort: Self-supervised meets active learning. In *Proceedings of the IEEE/CVF International Conference on Computer Vision*, pages 1631–1639, 2021. [1](#)
- [3] Samuel Budd, Emma C Robinson, and Bernhard Kainz. A survey on active learning and human-in-the-loop deep learning for medical image analysis. *Medical Image Analysis*, 71: 102062, 2021. [1](#)
- [4] Zhaowei Cai, Avinash Ravichandran, Subhransu Maji, Charles Fowlkes, Zhuowen Tu, and Stefano Soatto. Exponential moving average normalization for self-supervised and semi-supervised learning. In *Proceedings of the IEEE/CVF Conference on Computer Vision and Pattern Recognition*, pages 194–203, 2021. [5](#), [1](#)
- [5] Mathilde Caron, Hugo Touvron, Ishan Misra, Hervé Jégou, Julien Mairal, Piotr Bojanowski, and Armand Joulin. Emerging properties in self-supervised vision transformers. In *Proceedings of the IEEE/CVF international conference on computer vision*, pages 9650–9660, 2021. [1](#)
- [6] Yao-Chun Chan, Mingchen Li, and Samet Oymak. On the marginal benefit of active learning: Does self-supervision eat its cake? In *ICASSP 2021-2021 IEEE International Conference on Acoustics, Speech and Signal Processing (ICASSP)*, pages 3455–3459. IEEE, 2021. [1](#)
- [7] Ting Chen, Simon Kornblith, Mohammad Norouzi, and Geoffrey Hinton. A simple framework for contrastive learning of visual representations. In *International conference on machine learning*, pages 1597–1607. PMLR, 2020. [1](#)
- [8] Ting Chen, Simon Kornblith, Kevin Swersky, Mohammad Norouzi, and Geoffrey E Hinton. Big self-supervised models are strong semi-supervised learners. *Advances in neural information processing systems*, 33:22243–22255, 2020. [1](#), [2](#)
- [9] Gui Citovsky, Giulia DeSalvo, Claudio Gentile, Lazaros Karydas, Anand Rajagopalan, Afshin Rostamizadeh, and Sanjiv Kumar. Batch active learning at scale. *Advances in Neural Information Processing Systems*, 34:11933–11944, 2021. [2](#)
- [10] Cody Coleman, Christopher Yeh, Stephen Mussmann, Baharan Mirzasoleiman, Peter Bailis, Percy Liang, Jure Leskovec, and Matei Zaharia. Selection via proxy: Efficient data selection for deep learning. In *International Conference on Learning Representations*, 2019. [1](#), [2](#)
- [11] Jia Deng, Wei Dong, Richard Socher, Li-Jia Li, Kai Li, and Li Fei-Fei. Imagenet: A large-scale hierarchical image database. In *2009 IEEE conference on computer vision and pattern recognition*, pages 248–255. Ieee, 2009. [1](#), [5](#)
- [12] Zeyad Ali Sami Emam, Hong-Min Chu, Ping-Yeh Chiang, Wojciech Czaja, Richard Leapman, Micah Goldblum, and Tom Goldstein. Active learning at the imagenet scale. *arXiv preprint arXiv:2111.12880*, 2021. [2](#), [3](#)
- [13] Yarin Gal, Riashat Islam, and Zoubin Ghahramani. Deep bayesian active learning with image data. In *International Conference on Machine Learning*, pages 1183–1192. PMLR, 2017. [2](#)
- [14] Jean-Bastien Grill, Florian Strub, Florent Altché, Corentin Tallec, Pierre Richemond, Elena Buchatskaya, Carl Doersch, Bernardo Avila Pires, Zhaohan Guo, Mohammad Gheshlaghi Azar, et al. Bootstrap your own latent—a new approach to self-supervised learning. *Advances in Neural Information Processing Systems*, 33:21271–21284, 2020. [1](#)
- [15] Guy Hacohen, Avihu Dekel, and Daphna Weinshall. Active learning on a budget: Opposite strategies suit high and low budgets. In *International Conference on Machine Learning*, pages 8175–8195. PMLR, 2022. [2](#)
- [16] Kaiming He, Xiangyu Zhang, Shaoqing Ren, and Jian Sun. Deep residual learning for image recognition. In *Proceedings of the IEEE conference on computer vision and pattern recognition*, pages 770–778, 2016. [1](#), [5](#)
- [17] Kaiming He, Xinlei Chen, Saining Xie, Yanghao Li, Piotr Dollár, and Ross Girshick. Masked autoencoders are scalable vision learners. In *Proceedings of the IEEE/CVF conference on computer vision and pattern recognition*, pages 16000–16009, 2022. [1](#)
- [18] Andreas Kirsch, Joost Van Amersfoort, and Yarin Gal. Batchbald: Efficient and diverse batch acquisition for deep bayesian active learning. *Advances in neural information processing systems*, 32, 2019. [2](#)
- [19] Alex Krizhevsky, Geoffrey Hinton, et al. Learning multiple layers of features from tiny images. Technical Report TR-2009, University of Toronto, 2009. [5](#)
- [20] Ananya Kumar, Aditi Raghunathan, Robbie Jones, Tengyu Ma, and Percy Liang. Fine-tuning can distort pretrained features and underperform out-of-distribution. In *International Conference on Learning Representations*, 2022. [2](#), [5](#)
- [21] David D Lewis and Jason Catlett. Heterogeneous uncertainty sampling for supervised learning. In *Machine learning proceedings 1994*, pages 148–156. Elsevier, 1994. [2](#)
- [22] Xiaotong Li, Zixuan Hu, Yixiao Ge, Ying Shan, and Lingyu Duan. Exploring model transferability through the lens of potential energy. In *Proceedings of the IEEE/CVF International Conference on Computer Vision*, pages 5429–5438, 2023. [5](#)
- [23] Ze Liu, Yutong Lin, Yue Cao, Han Hu, Yixuan Wei, Zheng Zhang, Stephen Lin, and Baining Guo. Swin transformer: Hierarchical vision transformer using shifted windows. In *Proceedings of the IEEE/CVF International Conference on Computer Vision*, pages 10012–10022, 2021. [1](#)
- [24] Rafid Mahmood, Sanja Fidler, and Marc T Law. Low-budget active learning via wasserstein distance: An integer programming approach. In *International Conference on Learning Representations*, 2022. [2](#)
- [25] Mohammad Sadegh Norouzzadeh, Dan Morris, Sara Beery, Neel Joshi, Nebojsa Jojic, and Jeff Clune. A deep active learning system for species identification and counting in camera trap images. *Methods in ecology and evolution*, 12 (1):150–161, 2021. [1](#)
- [26] Maxime Oquab, Timothée Darcet, Théo Moutakanni, Huy Vo, Marc Szafranec, Vasil Khalidov, Pierre Fernandez,

- Daniel Haziza, Francisco Massa, Alaaeldin El-Nouby, et al. Dinov2: Learning robust visual features without supervision. *arXiv preprint arXiv:2304.07193*, 2023. [2](#)
- [27] Omkar M Parkhi, Andrea Vedaldi, Andrew Zisserman, and CV Jawahar. Cats and dogs. In *2012 IEEE conference on computer vision and pattern recognition*, pages 3498–3505. IEEE, 2012. [5](#)
- [28] Pengzhen Ren, Yun Xiao, Xiaojun Chang, Po-Yao Huang, Zhihui Li, Brij B Gupta, Xiaojiang Chen, and Xin Wang. A survey of deep active learning. *ACM computing surveys (CSUR)*, 54(9):1–40, 2021. [1](#)
- [29] Yi Ren, Shangmin Guo, Wonho Bae, and Danica J Sutherland. How to prepare your task head for finetuning. In *The Eleventh International Conference on Learning Representations*, 2022. [4](#)
- [30] Tobias Scheffer, Christian Decomain, and Stefan Wrobel. Active hidden markov models for information extraction. In *International symposium on intelligent data analysis*, pages 309–318. Springer, 2001. [2, 5](#)
- [31] Ozan Sener and Silvio Savarese. Active learning for convolutional neural networks: A core-set approach. In *International Conference on Learning Representations*, 2018. [2](#)
- [32] Changjian Shui, Fan Zhou, Christian Gagné, and Boyu Wang. Deep active learning: Unified and principled method for query and training. In *International Conference on Artificial Intelligence and Statistics*, pages 1308–1318. PMLR, 2020. [2](#)
- [33] Samarth Sinha, Sayna Ebrahimi, and Trevor Darrell. Variational adversarial active learning. In *Proceedings of the IEEE/CVF International Conference on Computer Vision*, pages 5972–5981, 2019. [2](#)
- [34] Toan Tran, Thanh-Toan Do, Ian Reid, and Gustavo Carneiro. Bayesian generative active deep learning. In *International Conference on Machine Learning*, pages 6295–6304. PMLR, 2019. [2](#)
- [35] Ziting Wen, Oscar Pizarro, and Stefan Williams. Ntkcpl: Active learning on top of self-supervised model by estimating true coverage. *arXiv preprint arXiv:2306.04099*, 2023. [2](#)
- [36] Jae Oh Woo. Active learning in bayesian neural networks with balanced entropy learning principle. In *The Eleventh International Conference on Learning Representations*, 2022. [2](#)
- [37] Yichen Xie, Han Lu, Junchi Yan, Xiaokang Yang, Masayoshi Tomizuka, and Wei Zhan. Active finetuning: Exploiting annotation budget in the pretraining-finetuning paradigm. In *Proceedings of the IEEE/CVF Conference on Computer Vision and Pattern Recognition*, pages 23715–23724, 2023. [1, 2, 5](#)
- [38] Lin Yang, Yizhe Zhang, Jianxu Chen, Siyuan Zhang, and Danny Z Chen. Suggestive annotation: A deep active learning framework for biomedical image segmentation. In *International conference on medical image computing and computer-assisted intervention*, pages 399–407. Springer, 2017. [2](#)
- [39] Ofer Yehuda, Avihu Dekel, Guy Hacohen, and Daphna Weinshall. Active learning through a covering lens. In *Advances in Neural Information Processing Systems*, 2022. [2](#)
- [40] Donggeun Yoo and In So Kweon. Learning loss for active learning. In *Proceedings of the IEEE/CVF conference on computer vision and pattern recognition*, pages 93–102, 2019. [2](#)
- [41] Kaichao You, Yong Liu, Jianmin Wang, and Mingsheng Long. Logme: Practical assessment of pre-trained models for transfer learning. In *International Conference on Machine Learning*, pages 12133–12143. PMLR, 2021. [5](#)
- [42] Jifan Zhang, Yifang Chen, Gregory Canal, Stephen Mussmann, Yinglun Zhu, Simon Shaolei Du, Kevin Jamieson, and Robert D Nowak. Labelbench: A comprehensive framework for benchmarking label-efficient learning. *arXiv preprint arXiv:2306.09910*, 2023. [1, 2, 3, 5, 6](#)
- [43] Renyu Zhang, Aly A Khan, Robert L Grossman, and Yuxin Chen. Scalable batch-mode deep bayesian active learning via equivalence class annealing. In *The Eleventh International Conference on Learning Representations*, 2022. [2](#)

Feature Alignment: Rethinking Efficient Active Learning via Proxy in the Context of Pre-trained Models

Supplementary Material

8. Hyperparameters

Fine-tuning, linear probing then fine-tuning (LP-FT), and proxy model training all utilized the SGD with momentum optimizer, with a momentum value of 0.9. For fine-tuning and LP-FT, the batch size in the training stage is 128 and the batch size in the sample selection stage of the active learning is 512.

The hyper-parameters of fine-tuning are shown in table 6. For ImageNet, we adopted the fine-tuning parameters following the prior work [4]. Setting the learning rates separately for the classifier head and the backbone. For CIFAR-10, CIFAR-100, and Pets, we followed prior work [4] to set the learning rate of the classifier as 0.1 and to search other hyper-parameters. The hyper-parameters are detailed in table 6. The learning rate of the backbone was searched from (0.01, 0.05, 0.1, 0.3) and the weight decay from (0, 0.0001). Additionally, to maintain consistency in training iterations between fine-tuning and LP-FT, we set the number of fine-tuning epochs as the sum of linear probing and fine-tuning epochs in LP-FT training.

Dataset	Learning Rate		Training Epochs	Weight Decay
	Classifier	Backbone		
ImageNet	0.1	0.01	50	0.0001
CIFAR-10	0.1	0.1	130	0
CIFAR-100	0.1	0.05	150	0
Pets	0.1	0.1	140	0

Table 6. The hyper-parameters of the fine-tuning.

For the LP-FT hyper-parameters, we conducted a search within the following ranges: (0.01, 0.1) for the classifier’s learning rate, (0.01, 0.05, 0.1, 0.3) for the backbone’s learning rate, (0.05, 0.1, 0.5) for learning rate in linear-probing (LP) stage, and (0, 0.0001) for weight decay. Fine-tuning (FT) training epochs were set at 120. For ImageNet, linear probing (LP) training epochs were searched from (5, 10), while for other datasets, LP training epochs were explored from (5, 10, 20, 30). Given the numerous hyper-parameters in LP-FT, we sequentially search the backbone learning rate, classifier learning rate, weight decay, and LP training epochs. The final hyper-parameters are shown in table 7, where the weight decay is 0 and the learning rate in the LP stage is 0.5 across all datasets.

The proxy model was trained 50 epochs with a learning rate of 0.01 and the weight decay of 0. During the training stage, the batch size is 2048 and in the active learning stage,

Dataset	Learning Rate		Training Epochs	
	Classifier	Backbone	LP	FT
ImageNet	0.01	0.01	5	45
CIFAR-10	0.1	0.01	10	120
CIFAR-100	0.1	0.01	30	120
Pets	0.1	0.1	20	120

Table 7. The hyper-parameters of the linear-probing then fine-tuning.

the batch size is 16384.

9. Accuracy and Sample Savings

The accuracy and the equivalent non-active learning label amount of all active learning strategies on ImageNet, CIFAR-10, CIFAR-100 and Pets are shown in the fig. 9-fig. 22. The equivalent non-active learning label amount refers to the number of samples selected by a random baseline to achieve the same accuracy as active learning.

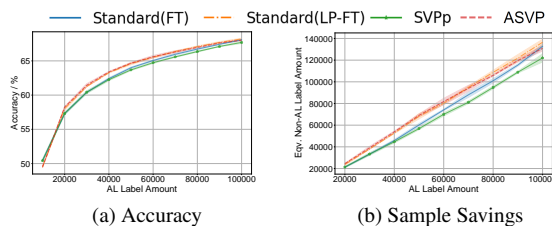


Figure 9. The accuracy and equivalent non-active learning label amounts of the standard method, SVPp and our method ASVP on the ImageNet, where active learning strategy is BADGE.

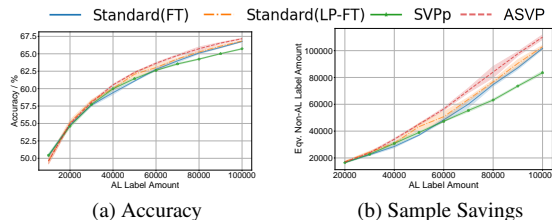


Figure 10. The accuracy and equivalent non-active learning label amounts of the standard method, SVPp and our method ASVP on the ImageNet, where active learning strategy is confidence.

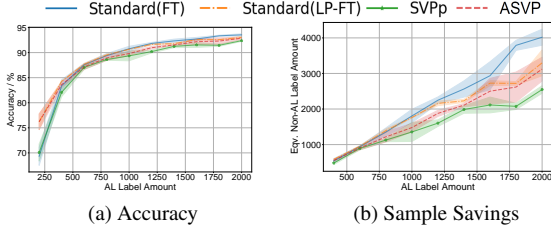


Figure 11. The accuracy and equivalent non-active learning label amounts of the standard method, SVPP and our method ASVP on the CIFAR-10, where active learning strategy is margin.

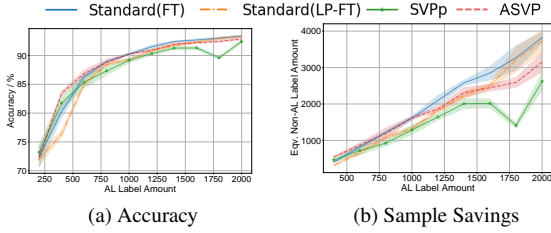


Figure 12. The accuracy and equivalent non-active learning label amounts of the standard method, SVPP and our method ASVP on the CIFAR-10, where active learning strategy is BADGE.

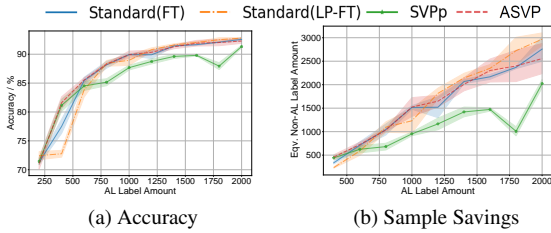


Figure 13. The accuracy and equivalent non-active learning label amounts of the standard method, SVPP and our method ASVP on the CIFAR-10, where active learning strategy is confidence.

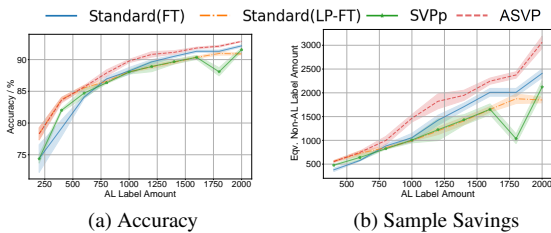


Figure 14. The accuracy and equivalent non-active learning label amounts of the standard method, SVPP and our method ASVP on the CIFAR-10, where active learning strategy is activeft(al).

10. Computation Time

The time for standard active learning, SVPP and ASVP on V100 GPU is presented in table 8. The active learning setup, outlined in sec. 6.1, performs a total of 10 active learning iterations on CIFAR-10 and Pets, where 200 sam-

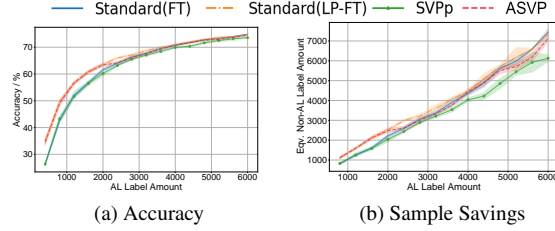


Figure 15. The accuracy and equivalent non-active learning label amounts of the standard method, SVPP and our method ASVP on the CIFAR-100, where active learning strategy is margin.

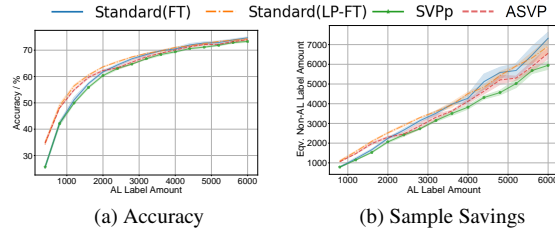


Figure 16. The accuracy and equivalent non-active learning label amounts of the standard method, SVPP and our method ASVP on the CIFAR-100, where active learning strategy is BADGE.

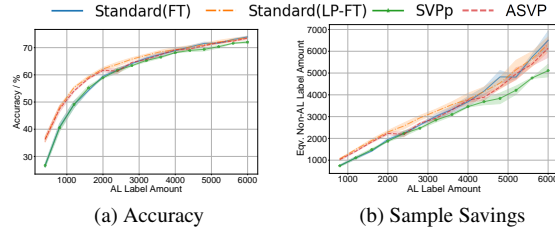


Figure 17. The accuracy and equivalent non-active learning label amounts of the standard method, SVPP and our method ASVP on the CIFAR-100, where active learning strategy is confidence.

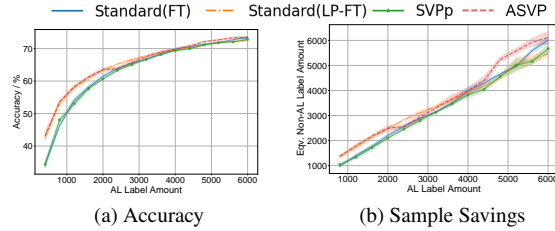


Figure 18. The accuracy and equivalent non-active learning label amounts of the standard method, SVPP and our method ASVP on the CIFAR-100, where active learning strategy is activeft(al).

ples are selected for each iteration. Regarding CIFAR-100, it spans 15 iterations, selecting 400 samples per iteration.

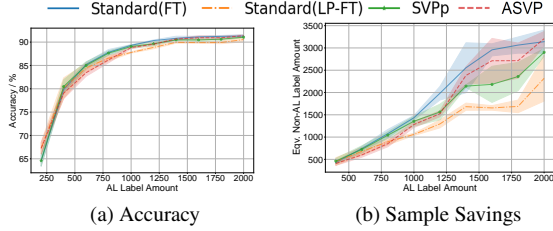


Figure 19. The accuracy and equivalent non-active learning label amounts of the standard method, SVPp and our method ASVP on the Pets, where active learning strategy is margin.

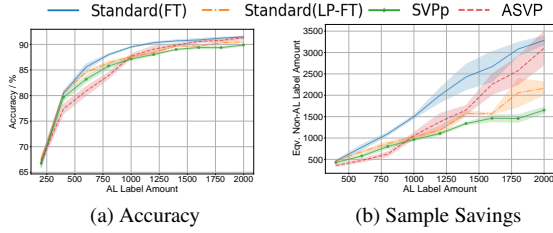


Figure 20. The accuracy and equivalent non-active learning label amounts of the standard method, SVPp and our method ASVP on the Pets, where active learning strategy is BADGE.

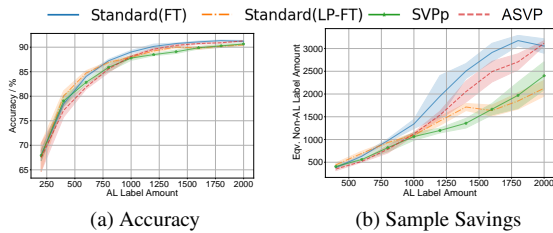


Figure 21. The accuracy and equivalent non-active learning label amounts of the standard method, SVPp and our method ASVP on the Pets, where active learning strategy is confidence.

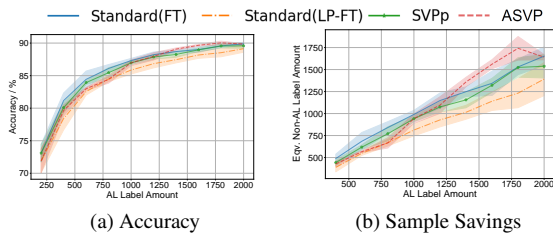


Figure 22. The accuracy and equivalent non-active learning label amounts of the standard method, SVPp and our method ASVP on the Pets, where active learning strategy is activeft(al).

11. Ablation Study

The results of ablation experiments with various active learning strategies are shown in table 9, table 10, table 11. Specifically, feature alignment refers to whether the ASVP method updates pre-computed features using fine-tuned

	CIFAR-10	CIFAR-100	Pets
Standard	1.4 hrs	5.5 hrs	1.5 hrs
SVPp	0.07 hrs	0.08 hrs	0.03 hrs
ASVP	0.14 hrs	0.14 hrs	0.05 hrs

Table 8. Sample selection time of standard active learning methods, SVPp, and our proposed method ASVP on CIFAR-10, CIFAR-100, and Pets. Experiments conducted on V100 GPU.

model features, while training alignment indicates the selection of the final model training method (FT or LP-FT) based on LogME-PED scores. In all ablation experiments, feature alignment consistently demonstrates notable improvements. Training alignment, except for the Pets dataset, exhibits enhancements.

Feature alignment	Training alignment	CIFAR-10	CIFAR-100	Pets
No	No	14.96±5.89	-2.11±0.85	-7.78±2.42
No	Yes	18.3±4.68	3.81±0.44	-15.61±1.93
Yes	No	30.34±2.06	2.25±2.25	13.93±5.21
Yes	Yes	33.67±0.84	8.16±1.98	6.1±5.59

Table 9. Ablation Study: Comparing the average sample saving ratio using the active learning strategy BADGE.

Feature alignment	Training alignment	CIFAR-10	CIFAR-100	Pets
No	No	-11.54±2.3	-14.43±2.49	2.4±7.25
No	Yes	-9.61±1.43	-7.86±2.16	-0.83±7.34
Yes	No	21.99±3.32	-7.19±1.69	18.05±2.92
Yes	Yes	23.92±5.16	-0.62±1.43	14.81±3.17

Table 10. Ablation Study: Comparing the average sample saving ratio using the active learning strategy confidence.

Feature alignment	Training alignment	CIFAR-10	CIFAR-100	Pets
No	No	-4.72±5.78	0.25±0.92	-11.63±6.85
No	Yes	-1.89±6.12	5.66±0.97	-14.76±6.74
Yes	No	24.62±1.31	5.86±2.24	-4.61±4.97
Yes	Yes	27.45±1.42	11.28±2.01	-7.74±4.81

Table 11. Ablation Study: Comparing the average sample saving ratio using the active learning strategy ActiveFT(al).

12. Postion of Updating pre-computed features

The ASVP method uses the difference in LogME-PED scores between consecutive active learning iterations to decide if updating pre-computed features is required. The absolute differences in LogME-PED scores are illustrated in

fig. 23, fig. 24, fig. 25. When the threshold is defined as 1, the updating positions are detailed in table 12.

	Updating Features	Position
ImageNet	No	$\geq 100k$
CIFAR-10	Yes	600
CIFAR-100	Yes	2000
Pets	Yes	800

Table 12. Positions of updating pre-computed features. The number of the PED convergence iterations is used to determine if updating pre-computed features is required. The positions are estimated by the absolute difference in LogME-PED scores between consecutive active learning iterations, where a difference smaller than 1 indicates an update.

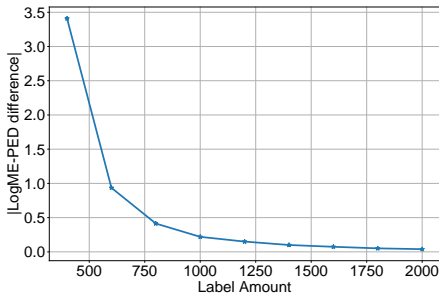


Figure 23. The absolute differences in LogME-PED scores between consecutive active learning iterations on CIFAR-10.

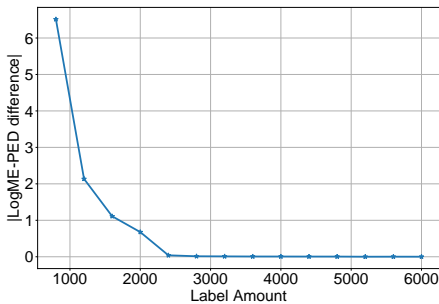


Figure 24. The absolute differences in LogME-PED scores between consecutive active learning iterations on CIFAR-100.

13. Computation Efficiency and Overall Cost

In fig. 29-fig. 37, we illustrate the overall costs (the labeling cost and the active learning training cost) and computational efficiency achieved by the standard active learning method, SVPP, and our proposed ASVP across different datasets. Compared to the existing efficient active learning method, SVPP, our method significantly improves the overall cost while maintaining the computational efficiency.

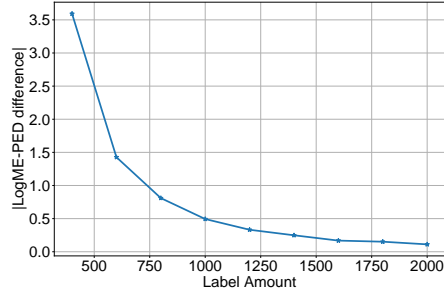


Figure 25. The absolute differences in LogME-PED scores between consecutive active learning iterations on Pets.

ASVP achieves comparable overall costs while significantly reducing active learning computation time compared to the standard active learning method. This effectively addresses the trade-off practitioners encounter between computational efficiency and total costs, offering confidence in the adoption of efficient active learning methods.

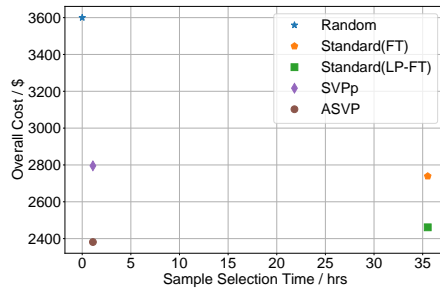


Figure 26. Computation efficiency and overall cost comparison of the standard active learning method, SVPP, and our method ASVP on ImageNet using margin sampling.

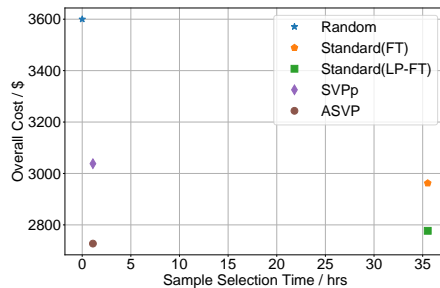


Figure 27. Computation efficiency and overall cost comparison of the standard active learning method, SVPP, and our method ASVP on ImageNet using BADGE.

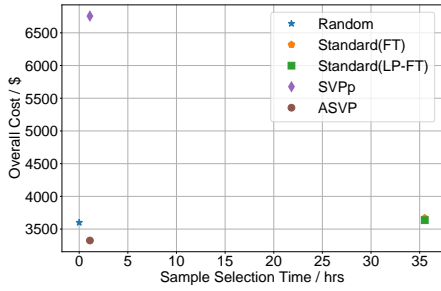


Figure 28. Computation efficiency and overall cost comparison of the standard active learning method, SVPP, and our method ASVP on ImageNet using confidence sampling.

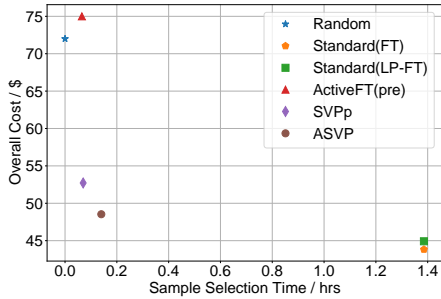


Figure 29. Computation efficiency and overall cost comparison of the standard active learning method, SVPP, and our method ASVP on CIFAR-10 using margin sampling.

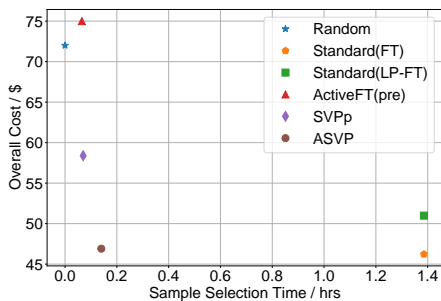


Figure 30. Computation efficiency and overall cost comparison of the standard active learning method, SVPP, and our method ASVP on CIFAR-10 using BADGE.

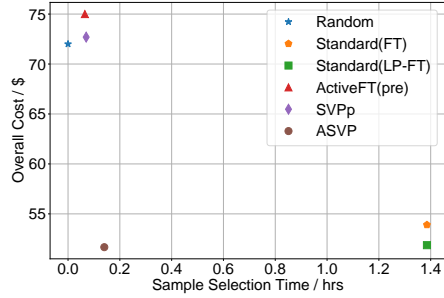


Figure 31. Computation efficiency and overall cost comparison of the standard active learning method, SVPP, and our method ASVP on CIFAR-10 using confidence sampling.

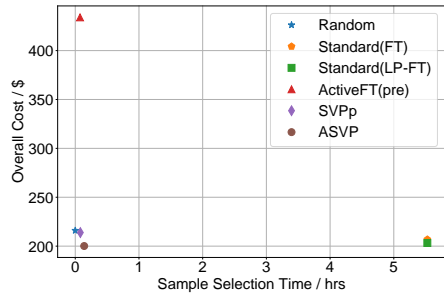


Figure 32. Computation efficiency and overall cost comparison of the standard active learning method, SVPP, and our method ASVP on CIFAR-100 using margin sampling.

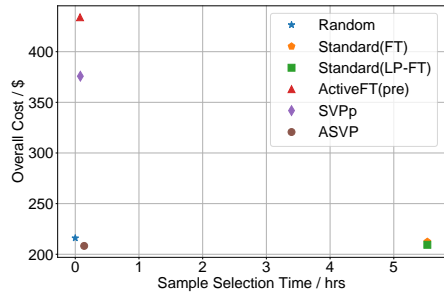


Figure 33. Computation efficiency and overall cost comparison of the standard active learning method, SVPP, and our method ASVP on CIFAR-100 using BADGE.

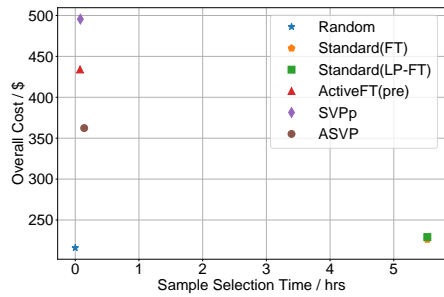


Figure 34. Computation efficiency and overall cost comparison of the standard active learning method, SVPP, and our method ASVP on CIFAR-100 using confidence sampling.

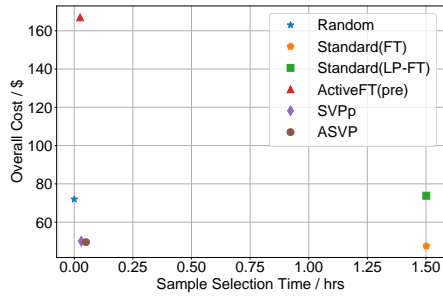


Figure 35. Computation efficiency and overall cost comparison of the standard active learning method, SVPP, and our method ASVP on Pets using margin sampling.

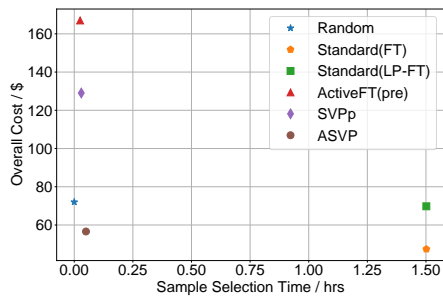


Figure 36. Computation efficiency and overall cost comparison of the standard active learning method, SVPP, and our method ASVP on Pets using BADGE.

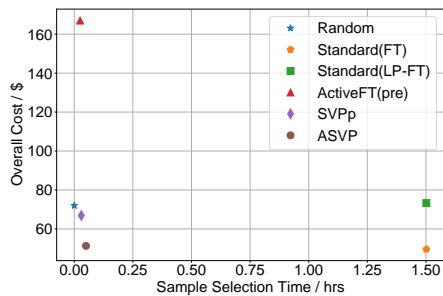


Figure 37. Computation efficiency and overall cost comparison of the standard active learning method, SVPP, and our method ASVP on Pets using confidence sampling.